Eur. Phys. J. D **37**, 371–375 (2006)
DOI: 10.1140/epjd/e2005-00326-y

THE EUROPEAN PHYSICAL JOURNAL D

Determination of probabilities of vacancy transfer from K to L shell using K X-ray intensity ratios

B. Ertuğral[1,a], G. Apaydın[1], A. Tekbıyık[1], E. Tıraşoğlu[1], U. Çevik[1], A.İ. Kobya[1], and M. Ertuğrul[2]

[1] Department of Physics, Faculty of Art and Sciences, Karadeniz Technical University, 61080 Trabzon, Turkey
[2] Department of Electrical and Electronic, Faculty of Engineering, Atatürk University, 25240 Ezurum, Turkey

Received 17 January 2005 / Received in final form 13 April 2005
Published online 13 December 2005 – © EDP Sciences, Società Italiana di Fisica, Springer-Verlag 2005

Abstract. K to L shell vacancy transfer probabilities (η_{KL}) for 26 elements in the atomic region $23 \leq Z \leq 57$ were determined by measuring the $I_{K\beta}/I_{K\alpha}$ intensity ratios. The targets were irradiated with γ-photons at 59.543 keV from ^{241}Am annular source. The K X-rays from different targets were detected with a high resolution Si(Li) detector. Theoretical values were calculated using the radiative and radiationless transition rates of these elements. The measured values of η_{KL} are compared with the theoretical values and data of others. The measurement vacancy transfer probabilities are least-square fitted to third-order polynomials to obtain analytical relations that represent these probabilities as a function of atomic number. The measured values of η_{KL} for V, Cr, Mn, Fe, Co, Ni, Cu, Zn, As, Se and Br are being reported here for the first time.

PACS. 32.80.Hd Auger effect and inner-shell excitation or ionization – 32.80.-t Photon interactions with atoms – 32.70.-n Intensities and shapes of atomic spectral lines

1 Introduction

When a single vacancy is created in an inner shell (e.g. the K shell), the vacancy is rapidly filled up by an electron coming from some higher (sub)shell, whereby in a radiative decay a photon and in a radiationless (Auger) decay an electron is emitted. Reliable accurate values of the decay probabilities are required in order to derive the vacancy creation from the observed photons or electrons. K to L shell vacancy transfer probability is defined as the number of L shell vacancies produced in the decay of one K shell vacancy through radiative or Auger transitions. Accurate experimental data regarding the vacancy transfer probability is important in many practical applications, such as nuclear electron capture, internal conversion of γ-rays, photoelectric effect, atomic processes leading to the emission of X-rays, Auger electrons and domestic computations for medical physics and irradiational processes.

In recent years, considerable efforts have been directed to the study of shell X-ray fluorescence (XRF) cross-sections, fluorescence yields and Coster-Kronig transitions. As a result of this effort, the K and L X-ray fluorescence cross-sections [1–6], K, L and M shell-subshell fluorescence yields [7,8], M shell XRF cross-sections and average fluorescence yield [9–11], Coster-Kronig transitions [12–14], the relative K and L shell X-ray intensities [15–17] data are now available in the literature.

The vacancy transfer probabilities in the atomic shell have been studied by a few authors [18–31]. Some of the authors have measured K to L shell vacancy transfer probabilities using different processes [29–31].

In this study, we measured K to L shell vacancy transfer probabilities for 26 elements in the atomic region $23 \leq Z \leq 57$ that are deduced by measuring K X-ray yields from targets excited by 59.543 keV photons and by using $I_{K\beta}/I_{K\alpha}$ intensity ratios. Finally the measured values of η_{KL} have been compared with all available data and the theoretical values deduced using the calculated radiative X-ray emission rates [32] and Auger transition rates [33] based on the relativistic Dirac-Hartree-Slater (RDHS) model.

2 Experimental

In this work, the studied elements were V, Cr, Mn, Fe, Co, Ni, Cu, Zn, As, Se, Br, Rb, Sr, Y, Zr, Nb, Mo, Ag, Cd, In, Sn, Sb, Te, I, Ba and La. High-purity (99%) samples of thickness from 15 to 42 mg cm^{-2} were used for the preparation of the targets. The experimental arrangement is shown in Figure 1. In the experimental arrangement, 59.543 keV γ-rays emitted from 1.85 GBq ^{241}Am radioisotope source were detected by a calibrated Si(Li) detector (active area 13 mm^2, thickness 3 mm and Be window thickness 30 mm) with an energy resolution of

[a] e-mail: ertugral@ktu.edu.tr

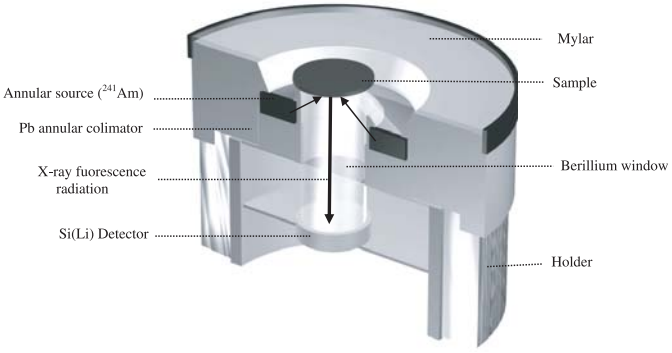

Fig. 1. Geometry of the experimental set-up.

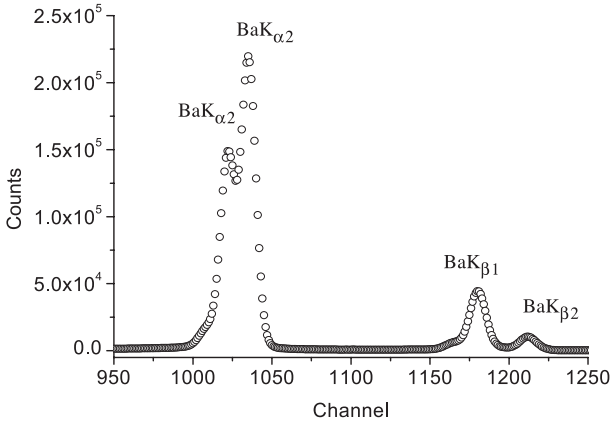

Fig. 2. Typical K X-ray spectrum for Ba.

approximately 160 eV at 5.96 keV. The output from the preamplifier, with pulse pile-up rejection capability, was fed to a multi-channel analyzer interfaced with a personal computer provided with suitable software for data acquisition and peak analysis. The live time was selected to be 5000 s for all elements. The samples were placed at a 45° angle with respect to the direct beam and fluorescent X-rays emitted 90° to the detector. A typical K X-ray spectrum for Ba is shown in Figure 2.

3 Data analysis

The experimental K to L total vacancy transfer probabilities, η_{KL}, were evaluated from [34]

$$\eta_{KL} = \frac{2 - \omega_K}{1 + (I_{K\beta}/I_{K\alpha})} \tag{1}$$

where ω_K is the fluorescence yield of the K shell [35] and $I_{K\beta}/I_{K\alpha}$ are the intensity ratios of the K X-rays. The $I_{K\beta}/I_{K\alpha}$ intensity ratio is obtained from [31]

$$\frac{I_{K\beta}}{I_{K\alpha}} = \frac{N_{K\beta}}{N_{K\alpha}} \frac{\beta_{K\alpha}}{\beta_{K\beta}} \frac{\varepsilon_{K\alpha}}{\varepsilon_{K\beta}} \tag{2}$$

where $N_{K\beta}$ and $N_{K\alpha}$ are the net counts under the K_β and K_α peaks, $\beta_{K\beta}$ and $\beta_{K\alpha}$ are the self-absorption correction

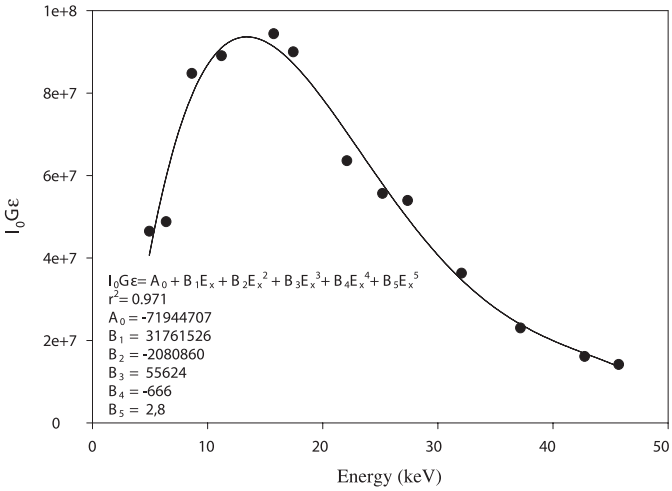

Fig. 3. $I_0G\varepsilon$ variation of energy.

factor for energies of K_β and K_α peaks. The factor β can be written as

$$\beta = \frac{1 - \exp\left[-\left(\mu_{inc}/\sin\theta + \mu_{emt}/\sin\phi\right)t\right]}{\left(\mu_{inc}/\sin\theta + \mu_{emt}/\sin\phi\right)t} \tag{3}$$

where μ_{inc} and μ_{emt} are the total mass absorption coefficients (from XCOM [36]) of target material at the incident photon energy and at the emitted average K_α and K_β X-ray energy [37] and t is the thickness of the target in g cm^{-2}, θ and ϕ are the angles of incident photon and emitted X-rays with respect to the normal at the surface of the sample.

$\varepsilon_{K\beta}$ and $\varepsilon_{K\alpha}$ are the detector efficiencies at the energies of the K X-ray energies have been evaluated using the equation

$$\varepsilon_{Ki} = \frac{N_{Ki}}{I_0 G \beta_{Ki} m_i \sigma_{Ki}} \tag{4}$$

where N_{Ki} and β_{Ki} have the same meaning as in equation (2). The term I_0 is the intensity of exciting radiation, G is the geometry factor, m_i is the mass of the element in the sample (g cm^{-1}) and the absolute efficiency ε of the X-ray detector was determined by collecting the K X-ray spectra of samples of V, Fe, Zn, Se, Zr, Mo, Ag, Sn, Te, Ba, Nd, Gd and Dy. Theoretical values of σ_{Ki} K X-ray production cross-sections were calculated using the equation

$$\sigma_{Ki} = \sigma_K^P \, \omega_K \, f_{Ki} \tag{5}$$

where σ_K^P is the K shell photoionization cross-section [38], and f_{Ki} is the fractional X-ray emission rate [39]. The measured variation of $I_0G\varepsilon$ as a function of the mean K X-ray energy is as shown in Figure 3.

Theoretical calculations were made according to our previous paper [31].

4 Result and discussion

The measured values of the K to L shell vacancy transfer probability, η_{KL}, for 26 elements, namely, V, Cr, Mn, Fe,

Table 1. Comparison of experimental and theoretical results for K to L shell vacancy transfer probability.

Z	Elements	η_{KL}					
		Present exp.	Fitted exp. values	Theoretical values	Other experimental values		
					Ref. [29]	Ref. [30]	Ref. [31]
23	V	1.544 ± 0.061	1.587	1.549	–	–	–
24	Cr	1.509 ± 0.044	1.550	1.515	–	–	–
25	Mn	1.467 ± 0.044	1.514	1.481	–	–	–
26	Fe	1.453 ± 0.042	1.479	1.448	–	–	–
27	Co	1.415 ± 0.057	1.445	1.416	–	–	–
28	Ni	1.394 ± 0.042	1.412	1.384	–	–	–
29	Cu	1.361 ± 0.041	1.380	1.354	–	–	–
30	Zn	1.330 ± 0.040	1.349	1.324	–	–	–
31	Ga	–	1.319	1.295	–	–	–
32	Ge	–	1.290	1.267	–	–	–
33	As	1.238 ± 0.037	1.262	1.241	–	–	–
34	Se	1.204 ± 0.036	1.235	1.215	–	–	–
35	Br	1.200 ± 0.048	1.209	1.190	–	–	–
36	Kr	–	1.184	1.166	–	–	–
37	Rb	1.123 ± 0.045	1.160	1.143	1.12	–	–
38	Sr	1.104 ± 0.055	1.137	1.122	1.10	–	–
39	Y	–	1.115	1.101	1.07	–	–
40	Zr	1.064 ± 0.032	1.094	1.081	1.03	–	–
41	Nb	1.042 ± 0.031	1.074	1.063	1.02	–	–
42	Mo	1.026 ± 0.041	1.055	1.045	1.02	–	–
43	Tc	–	1.037	1.028	–	–	–
44	Ru	–	1.020	1.012	–	–	–
45	Rh	–	1.004	0.998	–	–	–
46	Pd	0.990 ± 0.043	0.989	0.984	–	1.028	–
47	Ag	0.967 ± 0.029	0.975	0.971	–	0.995	–
48	Cd	0.962 ± 0.038	0.962	0.958	–	0.968	–
49	In	0.950 ± 0.028	0.950	0.947	–	0.957	–
50	Sn	0.943 ± 0.037	0.938	0.937	–	0.928	–
51	Sb	0.924 ± 0.037	0.928	0.927	–	0.912	–
52	Te	0.923 ± 0.046	0.919	0.918	–	0.909	0.908
53	I	0.917 ± 0.036	0.911	0.909	–	0.898	–
54	Xe	–	0.904	0.902	–	–	–
55	Cs	–	0.897	0.894	–	0.887	–
56	Ba	0.882 ± 0.026	0.892	0.888	–	–	0.905
57	La	0.873 ± 0.035	0.888	0.882	–	–	0.892

Co, Ni, Cu, Zn, As, Se, Br, Rb, Sr, Y, Zr, Nb, Mo, Ag, Cd, In, Sn, Sb, Te, I, Ba and La are listed in Table 1 with the theoretical and other experimental values. The overall error in the present measurements is estimated to be less than 8%. This error is attributed to the uncertainties in different parameters used to deduce η_{KL} values; namely, the error in the area evaluation under the K_α and K_β X-ray peak ($\leq$3%), in the absorption correction factor ratio ($\leq$2%), the product $I_0 G \varepsilon$ ($\leq$5–7%) and other systematic errors ($\leq$2–3%).

Earlier, Puri et al. [29] have measured the same quantity in the atomic region $37 \leq Z \leq 42$ at 5.96 and 22.6 keV energies using the same method. Şimşek et al. [30] determined K to L shell vacancy transfer probabilities for nine elements in the atomic region $46 \leq Z \leq 55$ measuring the L X-ray yields from targets excited by 5.96 and 59.5 keV photons. Ertuğral et al. [31] measured K to L shell vacancy transfer probabilities using intensity ratio of K_α and L_x total X-rays for some elements in the atomic region $52 \leq Z \leq 68$. In addition, Puri et al. [22] have calculated and fitted η_{KL} versus atomic number Z and also fitted coefficients for probabilities of vacancy transfer from K to L_1, K to L_2, K to L_3, K to L (average), L_1 to M, L_2 to M and L_3 to M shells. The values of the probabilities of vacancy transfer from the K to the L_1, L_2 and L_3 shells (η_{KL}) for elements in the atomic range $20 \leq Z \leq 94$ have been calculated by Rao et al. [18]. In these calculations, the contributions due to Auger and radiative transitions were derived using the best fitted experimental data on the fluorescence yields and intensity

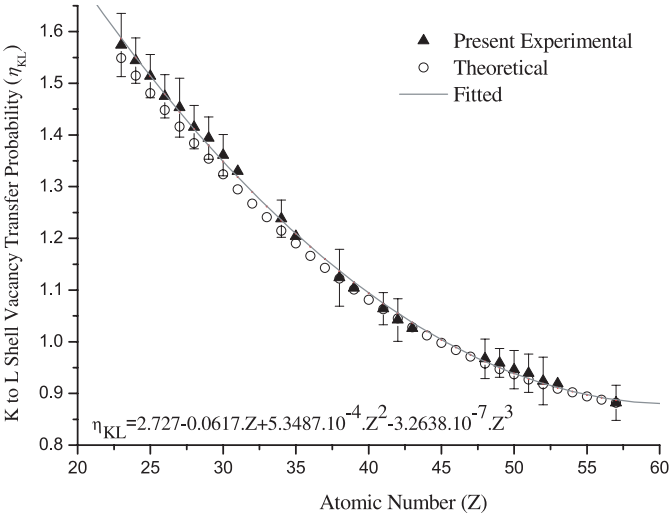

Fig. 4. η_{KL} versus atomic number (Z).

ratios of different components of KLX ($X = L$; M; N, etc.) Auger electrons and K X-rays currently available.

In earlier measurements [29,30], the authors used two radioisotope sources for excitation of targets. The method is based on the number of L X-rays produced at the photon excitation energy below the K edge and at the excitation energy above the K edge, where the major contribution to L shell vacancies comes from the decay K shell vacancies. The other investigator's method [31] is based on the K_α and total L_x X-rays yields from the targets and used a radioisotope source for excitation targets. Their methods were needed to measure L X-ray cross-sections. Some authors [29,30] and the others [31] measured K to L shell vacancy transfer using L X-rays and K and L X-rays for elements, respectively. In the present work, we only used K X-ray line intensities to measure same quantity. K X-ray production cross-sections are higher than L X-ray production cross-sections for the same excitation energy. Besides, as shown in Figure 3, detector efficiency at K X-ray energy region (5−35 keV) is better than detector efficiency at the L X-ray energy region (0.5−7 keV) for medium atomic number elements. So, the present method allowed us to measure K to L shell vacancy transfer probability for medium atomic number elements with much more accuracy.

Our experimental values were fitted to a third-order polynomial as a function of atomic number Z ($\Sigma A_n Z^n$) and fitted values of the K to L shell vacancy transfer probability listed in Table 1. These values have been plotted as a function of the atomic number and are shown in Figure 4. The fitted coefficients are also presented in Figure 4. Using these fitted values, the required experimental K to L shell vacancy transfer probability for individual elements can be obtained for comparison and the fit will be valid in the atomic range $23 \leq Z \leq 57$.

The experimental results alongside the theoretically calculated values are represented graphically as vacancy transfer probabilities versus atomic numbers in Figure 4. The values of the η_{KL} decrease as the atomic number increases. It can be seen from Table 1 and Figure 4 that our measurement values are in good agreement, within experimental uncertainties, with the calculated theoretical values for elements $23 \leq Z \leq 57$. Experimental values are generally lower than theoretical results. One of the reasons for this may be the chemical effect that occurred because of imperfections and impurities of the samples. The agreement between the present results and theoretical predictions are within the range 0.4−1.98% for K to L shell vacancy transfer probability.

In the calculated values, the radiative transition rates were taken from Scofield [32] and the radiationless (Auger) transition rates were taken from Chen et al. [33].

Our experimental values were compared with other experimental values. Present results show that agreement between present and theoretical values are better than earlier experimental values for many elements. Present good agreement with theoretical values leads to the conclusion that the present method will be beneficial for determining vacancy transfer probability in medium atomic numbers and satisfactory for many other applications employing the fundamental parameter approach.

The best of our knowledge there are no reports regarding the measurements of vacancy transfer probabilities of K to L shell for V, Cr, Mn, Fe, Co, Ni, Cu, Zn, As, Se and Br elements.

This work was done with the support of the Karadeniz Technical University Research Fund under Project No(s). 2002.111.1.4.

References

1. G. Budak, A. Karabulut, L. Demir, Y. Şahin, Phys. Rev. A **60**, 2015 (1999)
2. E. Tıraşoğlu, U. Çevik, B. Ertuğral, Y. Atalay, A.İ. Kobya, Rad. Phys. Chem. **60**, 11 (2001)
3. R.P. Garg, S. Puri, D. Mehta, J.S. Shahi, M.L. Garg, N. Singh, P.C. Mangal, P.N. Trehan, Nucl. Instrum. Meth. B **72**, 147 (1992)
4. E. Tıraşoğlu, U. Çevik, B. Ertuğral, G. Apaydın, M. Ertuğrul, A.İ. Kobya, Eur. Phys. J. D **26**, 231 (2003)
5. O. Dogan, O. Şimşek, U. Turgut, M. Ertuğrul, Phys. Scr. **56**, 580 (1997)
6. A. Kaya, M. Ertuğrul, J. Electron Spectrosc. **130**, 111 (2003)
7. O. Şimşek, O. Doğan, U. Turgut, M. Ertuğrul, Rad. Phys. Chem. **65**, 27 (2002)
8. M. Ertuğrul, Nucl. Instrum. Meth. B **124**, 475 (1997)
9. S. Puri, D. Mehta, N. Singh, P.C. Mangal, P.N. Trehan, Nucl. Instrum. Meth. B **49**, 319 (1993)
10. M. Ertuğrul, E. Tırasoğlu, Y. Kurucu, S. Erzenoğlu, R. Durak, Y. Şahin, Nucl. Instrum. Meth. B **108**, 18 (1996)
11. G. Apaydın, E. Tıraşoğlu, U. Çevik, B. Ertuğral, H. Baltaş, M. Ertuğrul, A.İ. Kobya, Rad. Phys. Chem. **72**, 549 (2005)
12. M. Ertuğrul, Appl. Radiat. Isot. **57**, 63 (2002)
13. M. Ertuğrul, J. Quant. Spect. RA **72**, 567 (2002)
14. O. Şimşek, Phys. Rev. A **62**, 052517 (2001)
15. M. Ertuğrul, O. Şimşek, J. Phys. B **35**, 601 (2002)

16. M. Ertuğrul, O. Söğüt, O. Şimşek, E. Büyükkasap, J. Phys. B **34**, 909 (2001)
17. O. Doğan, O. Şimşek, U. Turgut, M. Ertuğrul, J. Radio. Nucl. Chem. **232**, 143 (1998)
18. V.P. Rao, M.H. Chen, B. Crasemann, Phys. Rev. A **5**, 997 (1972)
19. M. Ertuğrul, O. Doğan, O. Şimşek, Rad. Phys. Chem. **49**, 221 (1997)
20. M. Ertuğrul, J. Phys. B: At. Mol. Opt. Phys. **28**, 4037 (1995)
21. M. Ertuğrul, J. Anal. At. Spectrom. **17**, 64 (2002)
22. S. Puri, D. Metha, B. Chand, N. Singh, J.H. Hubbell, P.N. Trehan, Nucl. Inst. Meth. B **83**, 21 (1993)
23. M. Ertuğrul, O. Doğan, O. Şimşek, Rad. Phys. Chem. **49**, 221 (1997)
24. M. Ertuğrul, J. Phys.: At. Mol. Opt. Phys. **36**, 2275 (2003)
25. S. Puri, D. Metha, B. Chand, N. Singh, P.N. Trehan, Nucl. Instrum. Meth. B. **74**, 347 (1993)
26. H.S. Sahota, R. Singh, N.P.S. Sidhu, X-Ray Spectrom. **17**, 99 (1988)
27. M. Ertuğrul, J. Anal. At. Spectrom. **16**, 771 (2001)
28. O. Şimşek, J. Phys. B. **35**, 1045 (2002)
29. S. Puri, D. Mehta, B. Chand, S. Nirmal, P.N. Trehan, Nucl. Instrum. Meth. B **73**, 443 (1993)
30. O. Şimşek, D. Karagoz, M. Ertuğrul, Spect. Acta Part B **58**, 1859 2003
31. B. Ertuğral, U. Çevik, E. Tirasoğlu, A.İ. Kobya, M. Ertuğrul, O. Doğan, J. Quant. Spect. RA **78**, 163 (2003)
32. J.H. Scofield, At. Data Tab. **14**, 121 (1974)
33. M.H. Chen, B. Crasemann, H. Mark, At. Data Nucl. Data Tab. **24**, 13 (1979)
34. E. Schönfeld, H. Janben, Nucl. Instrum. Meth. A **369**, 527 (1996)
35. W. Bambynek, *Molecules and Solids A Meisel*, Leipzig, DDR Paper P I. (1984)
36. M.J. Berger, J.H. Hubbell, S.M. Seltzer, J.S. Coursey, D.S. Zucker, NİST Standart Reference Database 8 (XGAM) (1998)
37. E. Storm, I.H. Israel, Nucl. Data Tab. A **7**, 565 (1970)
38. J.H. Scofield, UCRL Report 51326 Lawrence Livermore Laboratory CA (1973)
39. N. Broll, X-Ray Spect. **15**, 271 (1986)